

Comparing the same-side “ridge” in CMS p - p angular correlations to RHIC p - p data

Thomas A. Trainor and David T. Kettler

CENPA 354290, University of Washington, Seattle, WA 98195

(Dated: March 22, 2019)

The CMS collaboration has recently reported the appearance of a same-side “ridge” structure in two-particle angular correlations from 7 TeV p - p collisions. The ridge in p - p collisions at 7 TeV has been compared to a ridge structure in more-central Au-Au collisions at 0.2 TeV interpreted by some as evidence for a dense, flowing QCD medium. In this study we make a detailed comparison between 0.2 TeV p - p correlations and the CMS results. We find that 7 TeV minimum-bias jet correlations are remarkably similar to those at 0.2 TeV, even to the details of the same-side peak geometry. Extrapolation of azimuth quadrupole systematics from 0.2 TeV suggests that the same-side ridge at 7 TeV is a manifestation of the azimuth quadrupole with amplitude enhanced by applied cuts.

PACS numbers: 12.38.Qk, 13.87.Fh, 25.75.Ag, 25.75.Bh, 25.75.Ld, 25.75.Nq

I. INTRODUCTION

The CMS collaboration has recently released the first study of angular correlations from p - p collisions at the Large Hadron Collider (LHC) [1]. A notable result is the appearance of a same-side “ridge” structure possibly related to the expected jet peak at the angular origin (intrajet correlations). The same-side ridge observed in p - p collisions at 7 TeV has been compared to a ridge structure observed in more-central Au-Au collisions at the Relativistic Heavy Ion Collider (RHIC) [2], interpreted by some as evidence for a dense, flowing QCD medium [3, 4]. The apparent correspondence suggests that a dense medium may also form in p - p collisions at 7 TeV. While the CMS result is intriguing one can ask whether it does signal novel physics in p - p collisions at LHC energies or whether it is simply an extrapolation of p - p phenomena previously observed at 0.2 TeV.

In the present study we make quantitative comparisons between CMS results at 7 TeV and correlation measurements at 0.2 TeV. Our general strategy is to extrapolate measured 0.2 TeV p - p correlations to 7 TeV via an energy dependence established below 0.2 TeV and then determine what other alterations of the extrapolated correlation structure are required to describe the 7 TeV CMS data, both minimum-bias data and with cuts applied.

The paper is arranged as follows. We briefly review the CMS results. We then describe general correlation analysis methods applied to nuclear collisions at RHIC. We review the systematics of angular correlations from 0.2 TeV p - p collisions. We then make detailed A-B comparisons between extrapolated 0.2 TeV p - p correlations and the CMS results at 7 TeV.

II. CMS CORRELATION ANALYSIS

The CMS analysis is directly related to correlation analysis previously carried out at the RHIC. In order to distinguish what is truly novel at the LHC it is important to establish the quantitative relationships among different analysis methods, and the p - p phenomenology that

has emerged from previous work at lower energies.

A. CMS analysis method

The CMS analysis is based on normalized pair densities

$$S_N = \frac{1}{N(N-1)} \frac{d^2 N^{signal}}{d\Delta\eta d\Delta\phi} \quad (1)$$

$$B_N = \frac{1}{N^2} \frac{d^2 N^{bkd}}{d\Delta\eta d\Delta\phi},$$

where for example N^{signal} is a pair number, to be distinguished from N , the number of (charged) particles in the angular acceptance. Pair densities S_N and B_N are equivalent to pair numbers \hat{n}_{ab} defined in Ref. [5, 6], with sibling-to-mixed pair ratios $\hat{r}_{ab} = \hat{n}_{ab,sib}/\hat{n}_{ab,mix}$ for 2D bins (a, b) on difference variables $\eta_\Delta = \eta_1 - \eta_2$ (pseudorapidity) and $\phi_\Delta = \phi_1 - \phi_2$ (azimuth). The CMS correlation measure is

$$R(\Delta\eta, \Delta\phi) = \left\langle (\langle N \rangle - 1) \left(\frac{S_N}{B_N} - 1 \right) \right\rangle_N \quad (2)$$

$$= (\langle N \rangle - 1) (\langle \hat{r} \rangle - 1),$$

with the correspondence to measure $\langle N \rangle (\langle \hat{r} \rangle - 1)$ of Refs. [5, 6] established in the second line. The correlation measure defined in Eq. (2) is directly proportional to the detector angular acceptance.

Event multiplicity selection strongly influences spectrum and correlation structure in p - p collisions, mainly by biasing the jet frequency per p - p collision [7]. In the CMS analysis p_t -integral angular correlations were obtained for minimum-bias data and for a cut on “offline tracks” $N_{trk} > 110$ ($p_t > 0.4$ GeV/c, $|\eta| < 2.4$) which corresponds to $\langle N_{trk} \rangle = 118$. The corresponding corrected angular density is $dN_{ch}/d\eta \approx 40$. The NSD density is $dN_{ch}/d\eta \approx 5.8$, with $\langle N_{trk} \rangle \approx 16$ [8]. The ratio of cut-selected to minimum-bias corrected multiplicity is then about 7. p_t -differential correlations were also obtained for specific p_t bins. p_t cuts should modify jet correlations and possibly the azimuth quadrupole amplitude.

B. CMS correlation measurements

The main results are briefly summarized here. The correlation histograms are discussed in more detail in Sec. V. The CMS study concluded that jet correlations are enhanced in high-multiplicity collisions. The away-side ridge (interjet correlations) is flat for $|\eta| < 1.5$, consistent with STAR measurements within the TPC acceptance $|\eta| < 1$ [5, 9]. A CMS breakdown of p - p angular correlation structure at the LHC can be compared with 200 GeV p - p phenomenology described in Sec. IV.

Several p_t cut intervals were defined. For $p_t \in [1, 3]$ GeV/c and high-multiplicity cut a same-side “ridge” is observed and assumed to be associated with the same-side 2D jet peak. No corresponding ridge is observed in PYTHIA data. The p_t and N_{ch} dependence of the same-side ridge is studied via ZYAM subtraction. The same-side ridge does not depend on charge combinations. A similar structure is observed for correlated γ s from π^0 decay. The observation of a same-side ridge in p - p collisions at 7 TeV and possible implications in the context of a same-side “ridge” in more-central RHIC A-A collisions are the featured results of the analysis.

III. ANALYSIS METHOD FOR THIS STUDY

In this section we review technical aspects of STAR correlation analysis applied to nuclear collisions at RHIC. Method details are provided in Refs. [5, 9–15].

A. Angular correlations on $(\eta_\Delta, \phi_\Delta)$

Two-particle angular correlations are defined on 4D momentum subspace $(\eta_1, \eta_2, \phi_1, \phi_2)$. In acceptance intervals where correlation structure is invariant on mean position (e.g. $\eta_\Sigma = \eta_1 + \eta_2$) angular correlations can be *projected by averaging* onto difference variables (e.g. $\eta_\Delta = \eta_1 - \eta_2$) without loss of information to form *angular autocorrelations* [6, 10]. The 2D subspace $(\eta_\Delta, \phi_\Delta)$ is then visualized. The notation x_Δ rather than Δx for difference variables is adopted to conform to mathematical notation conventions and to reserve Δx as a measure of the detector acceptance on parameter x . Angular correlations can be formed separately for like-sign (LS) and unlike-sign (US) charge combinations, as well as for the charge-independent (CI = LS + US) combination [5, 6].

B. Correlations on $\mathbf{y}_t \times \mathbf{y}_t$

2D correlations on p_t or transverse rapidity $y_t = \ln[(p_t + m_t)/m_\pi]$ (m_π for unidentified hadrons) are complementary to 4D angular correlations in 6D two-particle momentum space. y_t is preferred for visualizing correlation structure on transverse momentum. Similar to angular correlations, $y_t \times y_t$ correlations can be defined for LS

and US charge combinations but also for same-side (SS, $|\phi_\Delta| < \pi/2$) and away-side (AS, $\pi/2 < |\phi_\Delta| < \pi$) subregions of angular correlations. Different correlation mechanisms can be distinguished in the four subspaces [13–15].

C. Correlation measures

We measure $\Delta\rho/\sqrt{\rho_{ref}} = \rho_0 (\langle r \rangle - 1)$ with $\langle r \rangle$ the sibling/mixed pair ratio. Assuming a uniform particle density within the angular acceptance $\langle N_{ch} \rangle = \Delta\eta\Delta\phi\rho_0$, where ρ_0 is the average 2D angular density within the acceptance. The sibling and mixed pair numbers are normalized to unit integral, and pair ratio r is averaged over kinematic bins (e.g. multiplicity, p_t , vertex position).

For our initial angular correlation measurements we adopted $\langle N_{ch} \rangle (\langle r \rangle - 1)$ as the correlation measure [5, 6]. That *per-particle* measure was an improvement over conventional *per-pair* measure (correlation function) $C \leftrightarrow \langle r \rangle$ or $\langle r \rangle - 1 \rightarrow \Delta\rho/\rho_{ref}$ ($\Delta\rho$ is the correlated-pair density and ρ_{ref} is the reference- or mixed-pair density) since it eliminated a trivial $1/N_{ch}$ trend common to all per-pair measures [10]. However, such extensive measures depend directly on the specific detector angular acceptance.

The corresponding intensive correlation measure is $(1/\Delta\eta\Delta\phi) \langle N_{ch} \rangle (\langle r \rangle - 1) = \rho_0 (\langle r \rangle - 1) \rightarrow \Delta\rho/\sqrt{\rho_{ref}}$, assuming a uniform single-particle density within the angular acceptance and factorization of the reference-pair density. $\Delta\rho/\sqrt{\rho_{ref}}$, a form of Pearson’s normalized covariance [10], is invariant under the combination of uncorrelated parts, therefore should not change with *linear superposition* of N-N collisions. The measure is independent of angular acceptance provided the underlying physical mechanisms are uniform across the acceptance.

D. A-B comparisons

Histograms for this study were binned as 25x28 on $(\eta_\Delta, \phi_\Delta)$ to match the CMS binning. Detailed comparisons of contour lines between data and model functions then permit inference of model parameters from the CMS data. Inferred parameters are typically accurate to 10% for the simple structures in p - p correlations. The CMS palette includes 20 colors, whereas this study employs over 50 colors, causing significant differences in shading in some regions. An attempt was made to insure that the intervals spanned by vertical scales are nearly the same for the model and the CMS plot in each comparison, although the offsets may differ due to analysis details.

IV. 0.2 TEV p-p ANGULAR CORRELATIONS

p - p and A-A angular correlations at RHIC have been extensively studied by the STAR collaboration [5, 6, 9, 11–15]. Those results should provide an essential reference for the CMS measurements at 7 TeV.

A. Two-component angular correlations

Spectra and correlations in nuclear collisions can be decomposed (near mid-rapidity) into soft and hard components, denoting respectively longitudinal fragmentation (diffractive dissociation) of projectile nucleons and transverse fragmentation of large-angle scattered partons [7, 13–16]. The hard-component fraction amounts to a few percent in p - p collisions [7] but increases to about 1/3 of the final-state yield in central Au-Au collisions [17].

B. Minijet phenomenology

Minijets play a key role in RHIC collisions [16, 18, 20, 28]. The history of minijets dates from UA1 observations in 1985 of jet production at $\sqrt{s} = 200$ GeV following pQCD cross-section predictions down to 5 GeV (background corrected to 3-4 GeV) [19]. Because of the parton spectrum structure (power law with lower cutoff at 3 GeV) the minimum-bias parton (jet) spectrum is dominated by 3 GeV jets [20]. Thus, correlations from 3 GeV minijets and from minimum-bias jets are effectively equivalent.

The interplay of correlations on $(\eta_\Delta, \phi_\Delta)$ and $y_t \times y_t$ for SS/AS angular subregions and LS/US sign combinations distinguishes soft- and hard-component correlation structure [13–15]. For instance, SS-US $y_t \times y_t$ correlations show clear *intrajet* structure extending down to 0.3 GeV/c with mode at $y_t = 2.7$ ($p_t \sim 1$ GeV/c), corresponding exactly when projected to the p - p p_t spectrum hard component first revealed in Ref. [7]. The SS-LS combination is dominated by HBT correlations appearing below 0.5 GeV/c, with negligible jet contribution.

AS-LS and AS-US correlations contain identical *interjet* contributions appearing above 0.7 GeV/c, also with mode at $y_t = 2.7$ ($p_t \sim 1$ GeV/c). The absence of charge dependence for AS jet structure is consistent with scattered partons (mainly gluons) having no charge correlation. The AS-US combination also shows a soft-component contribution below 0.5 GeV/c. Cuts on $y_t \times y_t$ in turn isolate corresponding elements of angular correlations. The combination provides a clear picture of local charge conservation in two orthogonal fragmentation processes plus like-sign quantum correlations (HBT) [13–15].

C. Correlation model functions

The soft component of angular correlations is modeled by a 1D Gaussian on η_Δ with r.m.s. width approximately 1. The model is assumed to be uniform on ϕ_Δ for simplicity. However, there are indications that the soft component is suppressed near $\phi_\Delta = 0$ as a result of local transverse-momentum conservation. The soft component falls within $p_t < 0.5$ GeV/c. Its amplitude decreases to zero with increasing centrality in A-A collisions. The soft

component is exclusively US pairs, reflecting local charge conservation during projectile-nucleon fragmentation.

The hard component consists of two parts, a SS 2D peak at the origin and an AS 1D peak on azimuth uniform on η_Δ (within the STAR TPC acceptance). The SS peak (intrajet correlations) is well modeled by a 2D Gaussian. The AS “ridge” (interjet correlations) can be modeled by a 1D Gaussian on azimuth centered at π (plus periodic image at $-\pi$ [21]). Except for p - p and most-peripheral A-A collisions the AS peak is more conveniently modeled as an AS dipole with form $\cos(\phi_\Delta - \pi)$, since for r.m.s. widths greater than 1.2 the higher Fourier components of the AS periodic peak array become negligible [21].

The combined model function [5, 9], which includes an azimuth quadrupole term $\cos(2\phi_\Delta)$ required to describe minimum-bias A-A angular correlations, is

$$\frac{\Delta\rho}{\sqrt{\rho_{ref}}} = A_0 + A_1 e^{-\frac{1}{2}\left\{\left(\frac{\phi_\Delta}{\sigma_{\phi_\Delta}}\right)^2 + \left(\frac{\eta_\Delta}{\sigma_{\eta_\Delta}}\right)^2\right\}} + A_2 e^{-\frac{1}{2}\left(\frac{\eta_\Delta}{\sigma_2}\right)^2} + A_D [1 + \cos(\phi_\Delta - \pi)]/2 + A_Q \cos(2\phi_\Delta), \quad (3)$$

where a narrow 2D exponential describing quantum correlations and electron pairs from γ conversions has been omitted for clarity. The dipole term in Eq. (3) is different in form from that in Ref. [9]. For p - p collisions the dipole term is replaced by a 1D Gaussian on azimuth at π with periodic image at $-\pi$. The SS 2D jet peak is also characterized as $\rho_0(b)j^2(\eta_\Delta, \phi_\Delta, b)$ within angular acceptance $(\Delta\eta, \Delta\phi) = (2, 2\pi)$ —the STAR TPC acceptance [17]. The corresponding CMS acceptance is $(4.8, 2\pi)$.

D. 200 GeV p - p model parameters

Figure 1 shows model results for 200 GeV NSD p - p collisions in the STAR intensive format (left panel) and in the CMS extensive format including the angular acceptance (right panel), the latter as in Ref. [5]. Results obtained directly from NSD p - p collisions [14, 15] are consistent with A-A collisions extrapolated to peripheral N-N collisions [9], providing a cross check of methods and data consistency. We treat the two cases as equivalent.

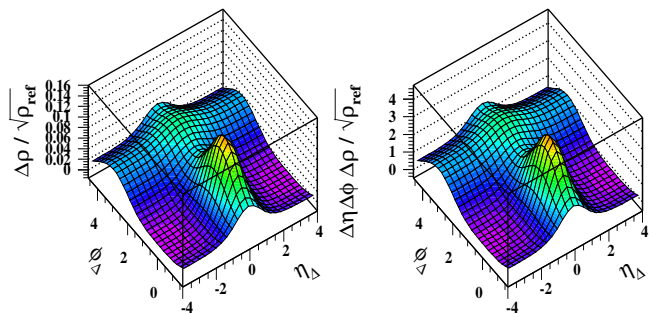


FIG. 1: Left: Model angular correlations representing 200 GeV NSD p - p collisions [14, 15]. Right: The same plot rescaled by the CMS angular acceptance $\Delta\eta\Delta\phi = 4.8 \times 2\pi$.

Measured 2D Gaussian parameters [9] are $A_1 = 0.058$, $\sigma_{\eta_\Delta} = 0.64$ and $\sigma_{\phi_\Delta} = 0.9$. The AS azimuth dipole amplitude is $A_D \sim 0.046$ (twice the value in Ref. [9] because of the different dipole definition). When modeled as a 1D Gaussian the AS peak amplitude remains 0.046, but with r.m.s. width 1.0. The amplitude of the 1D Gaussian on η_Δ is $A_2 = 0.023$ with $\sigma_2 = 1.0$. The quadrupole amplitude is $A_Q \sim 0.0005$.

Note that the minimum-bias SS 2D jet peak in p - p collisions is strongly elongated in the *azimuth* direction, with an approximate 3:2 aspect ratio [14, 15]. The strong ϕ elongation in p - p collisions contrasts with strong η elongation in more-central Au-Au collisions [5, 9].

E. Multiplicity dependence of the hard component

The p_t spectrum hard component in 200 GeV NSD p - p collisions is observed to scale nearly linearly (relative to the soft component) with N_{ch} as N_{ch} increases by a factor ten relative to the NSD value [7]. The spectrum hard component corresponds quantitatively to minijet correlations [17] and to pQCD-calculated fragment distributions [20]. The single-particle hard-component yield increases by a factor 50 as the particle multiplicity near mid-rapidity increases ten-fold. Equivalently, the jet frequency per event within one unit of η increases from 2% to nearly 100%. The jet frequency saturates at one jet (pair) per collision for large event multiplicities.

Corresponding jet angular correlations scale as follows. The mean jet fragment multiplicity (~ 2.5 , dominated by 3 GeV jets) does not change significantly with N_{ch} (the number of correlated pairs per jet is then fixed), but the jet frequency increases by a factor 50 with $10\times$ increase in N_{ch} , rising to one jet per event. Jet correlations measured by $\rho_0 j^2$ then scale up as $10 \times (50/10^2) = 5$, since pair ratio j^2 represents correlated pairs / reference pairs.

F. Collision-energy dependence

We observe that minijet correlations in the form $\rho_0(b) j^2(\eta_\Delta, \phi_\Delta, b)$ [22, 23] and the azimuth quadrupole in the form $\rho_0(b) v_2^2(b)$ [11, 24] (next subsection) scale approximately as $\log(\sqrt{s_{NN}}/\text{constant})$ below 200 GeV, where the constant is near 13.5 GeV. We therefore define

$$R(\sqrt{s_{NN}}) = \log(\sqrt{s_{NN}}/13.5 \text{ GeV}) / \log(200/13.5) \quad (4)$$

to represent collision-energy scaling of jets and quadrupole relative to 200 GeV [11]. Assuming the same scaling up to 7 TeV implies that both amplitudes should be larger by factor $\log(7000/13.5) / \log(200/13.5) \approx 2.3$ at 7 TeV than at 200 GeV.

The symbol R introduced in the CMS analysis should be distinguished from energy scaling factor $R(\sqrt{s})$ in Eq. (4) defined in Ref. [11] in connection with v_2 analysis.

G. Azimuth quadrupole systematics

The azimuth quadrupole, with form $\cos(2\phi_\Delta)$, is conventionally interpreted in A-A collisions as “elliptic flow,” a conjectured response to early development of large pressure gradients in non-central A-A collisions [25]. v_2 values inferred from 2D angular correlations and denoted $v_2\{2D\}$, which accurately exclude contributions from jets (“nonflow”), reveal systematic behavior inconsistent with hydro expectations, suggesting an alternative interpretation in terms of interacting gluonic fields [11, 24]. Although the azimuth quadrupole is not typically considered relevant to p - p collisions it may be relevant to the novel CMS results as demonstrated below.

An analysis of p_t -integral $v_2\{2D\}$ for Au-Au collisions at 62 and 200 GeV, combined with SPS $v_2\{EP\}$ data at 17 GeV, led to the following simple relation describing all p_t -integral $v_2\{2D\}$ data from 13.5 to 200 GeV [11]

$$\frac{\Delta\rho[2]}{\sqrt{\rho_{ref}}} = \rho_0(b) v_2^2\{2D\}(b) = 0.0045 R(\sqrt{s_{NN}}) \epsilon_{opt}^2 n_{bin}. \quad (5)$$

For 200 GeV NSD p - p collisions $n_{bin} = 1$ and we assume $\epsilon_{opt} \sim 0.3$ yielding $\rho_0 v_2^2 \sim 0.0005$. For the CMS analysis additional factors lead to $R_Q \equiv R(7 \text{ TeV}) \Delta\eta\Delta\phi 2\rho_0 v_2^2 = 2.3 \times 30 \times 2 \times 0.0005 = 0.07$ as the *predicted* quadrupole amplitude for minimum-bias p - p angular correlations consistent with CMS measure R .

The azimuth quadrupole in Au-Au collisions at RHIC energies is insensitive to charge-sign combinations. The amplitude for LS pairs is the same as that for US pairs [6].

The role of p - p collision centrality is of significant interest at the LHC [26]. Increasing multiplicity cuts should bias the p - p collision geometry to more-central collisions. The product $\epsilon_{opt}^2(b) n_{bin}(b)$ in Eq. (5) increases rapidly with increasing centrality in Au-Au collisions (50-fold increase) to a maximum for mid-central collisions, beyond which the rapidly decreasing eccentricity dominates [11]. That centrality trend for Au-Au collisions, independent of collision energy, suggests that with increasing multiplicity (centrality) $\rho_0 v_2^2$ for p - p may also increase substantially.

CMS p_t cuts relate to p_t -differential v_2 trends. Such trends have been measured for *marginal* $v_2\{2D\}(p_t, b)$ distributions on p_t at 200 GeV [12], but not for specific 2D bins on $y_t \times y_t$ equivalent to CMS p_t cuts. In Sec. V C we infer an empirical multiplicative factor for changes in the quadrupole amplitude due to multiplicity and/or p_t cuts from comparisons between the minimum-bias prediction $R_Q \sim 0.07$ and CMS cut-selected data. From that comparison we find no significant change in the quadrupole amplitude due to p_t cuts alone.

V. 7 TEV p-p ANGULAR CORRELATIONS

We compare our scaled 0.2 TeV angular correlation results to CMS 7 TeV results for minimum-bias and cut-selected data.

A. Minimum-bias angular correlations

For the extrapolation we assume the simplest case: $\log(\sqrt{s})$ scaling observed below 200 GeV continues to 7 TeV. We then scale all STAR minimum-bias 200 GeV angular correlation structure as $X(7 \text{ TeV}) = R(7 \text{ TeV}) 2\pi\Delta\eta X(0.2 \text{ TeV})$, with $R(7 \text{ TeV}) = 2.3$ and $\Delta\eta = 4.8$. The overall factor is about 70. The resulting model function in Fig. 2 (left panel) compares well with CMS minimum-bias results in the right panel, but only if the AS ridge amplitude is reduced by factor 0.6 (compare with Fig. 1). The AS amplitude reduction may be a consequence of the larger $4\pi \eta$ acceptance at 7 TeV compared to 200 GeV [20]. The AS reduction factor is retained for all subsequent comparisons. The large ϕ elongation (3:2) of the SS 2D peak observed in 200 GeV p - p collisions [15] apparently persists in 7 TeV collisions.

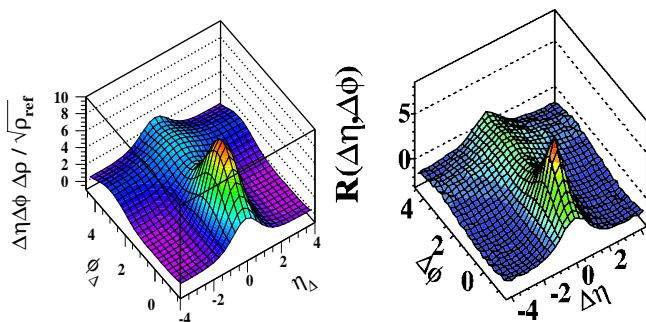


FIG. 2: Left: The function from Fig. 1 (left panel) rescaled by energy-dependent factor $R(7 \text{ TeV}) = 2.3$. Right: CMS angular correlations for minimum-bias 7 TeV p - p collisions [1].

B. High-multiplicity cut

By selecting high-multiplicity p - p collisions we expect to bias the jet frequency per event to larger frequencies [7]. Figure 3 (left panel) shows the model function in Fig. 2 (left panel) with the following changes: (i) The jet structure (SS 2D peak, AS ridge) is scaled up by factor 3, (ii) the SS peak ϕ width is reduced to 0.65 from 0.9 and the η width to 0.58 from 0.64, and (iii) the 1D η Gaussian is eliminated. The quadrupole component for this figure (not visible) is unchanged from Fig. 2 (minimum-bias $R_Q = 0.07$). The result compares well with CMS data in the right panel, with the exception of the narrow contribution from quantum correlations and electron pairs at the peak which is not included in the model.

Figure 4 shows the results in Fig. 3 with the vertical axis range reduced by a factor 5 to enhance details. Correspondence of the SS jet peaks near the base is evident. The AS ridge shows significant reduction in the data at larger η_Δ (lower panel) which is not included in the model function (upper panel) inferred within the STAR TPC acceptance.

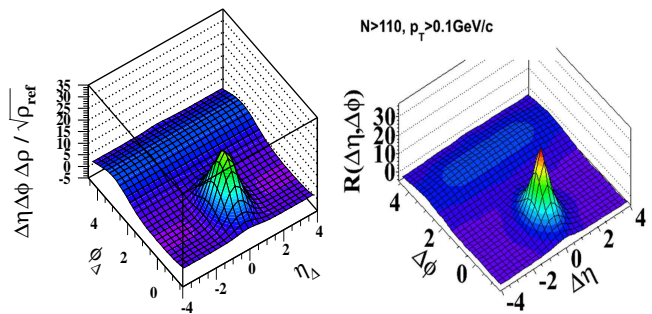


FIG. 3: Left: Model function from Fig. 2 (left panel) multiplied by factor 3, with SS peak narrowed and 1D η_Δ Gaussian removed. Right: CMS p_t -integral angular correlations for high-multiplicity 7 TeV p - p collisions [1].

The quadrupole amplitude has been increased by factor 6 for this figure (relative to the minimum-bias value) to $R_Q = 0.4$. The larger quadrupole amplitude changes the SS curvature at larger $|\eta_\Delta|$ from concave upward to concave downward (compare with Fig. 3 – left panel).

C. High-multiplicity plus high- p_t cuts

With high- p_t cuts we expect to eliminate some fraction of the jet contribution, to eliminate any remaining evidence of the soft component and possibly to further increase the quadrupole amplitude. Figure 5 (upper panel) shows the model in Fig. 4 (upper panel) with the following changes: (i) The ϕ width of the SS 2D peak is further reduced from 0.65 to 0.55 leading to a symmetric peak, (ii) The SS peak amplitude is reduced by factor 1/3 and AS ridge by factor 1/2 compared to the high-multiplicity cut alone (consequence of reduced p_t acceptance for jet-correlated pairs) and (iii) quadrupole amplitude remains the same as for the high-multiplicity cut alone— $R_Q = 0.4$ increased by factor 6 from minimum-bias 0.07. The comparison to CMS data in the lower panel shows good agreement, especially near the base of the SS 2D peak.

It is notable that the quadrupole amplitude remains the same in Figs. 4 and 5, but the jet structure in Fig. 5 is reduced in amplitude by factor 2-3 relative to the quadrupole amplitude. Because the vertical sensitivity in Fig. 5 is doubled the SS quadrupole structure (the “ridge”) becomes clearly visible there. Any change in the quadrupole amplitude with application of p_t cuts is not significant for these data. That conclusion appears to contradict what is inferred from the ZYAM analysis in Ref. [1]. ZYAM subtraction can be misleading [21].

VI. DISCUSSION

Minimum-bias jet structure at the LHC is remarkably similar to that at RHIC scaled up by a simple $\log(\sqrt{s})$ energy-dependence factor. Possible novelty arises with

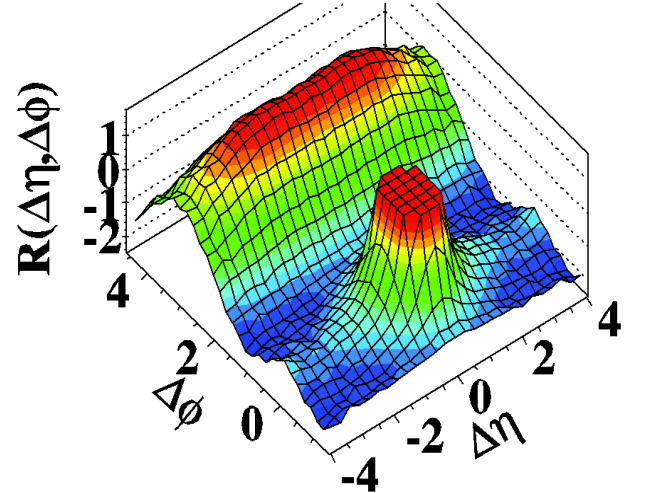
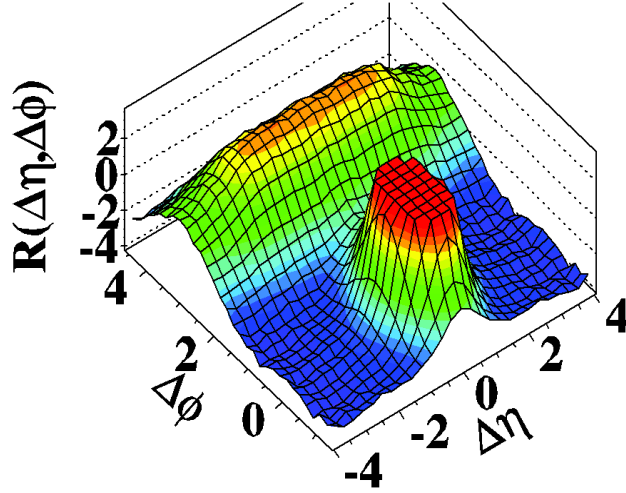
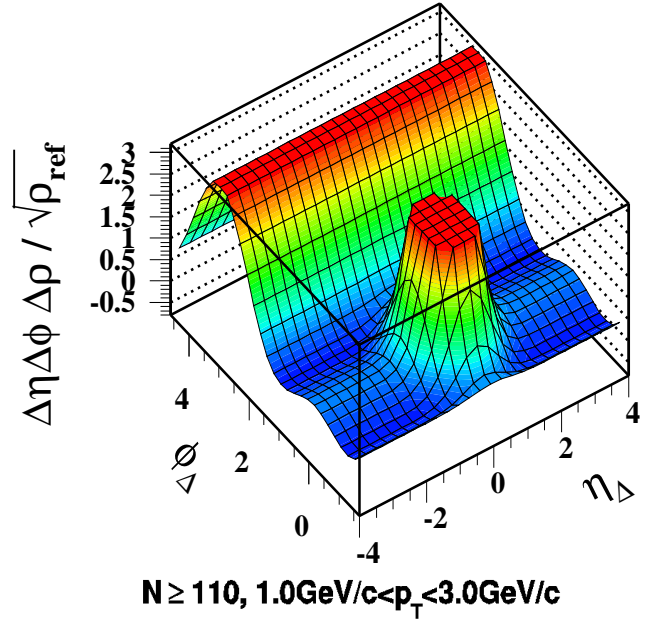
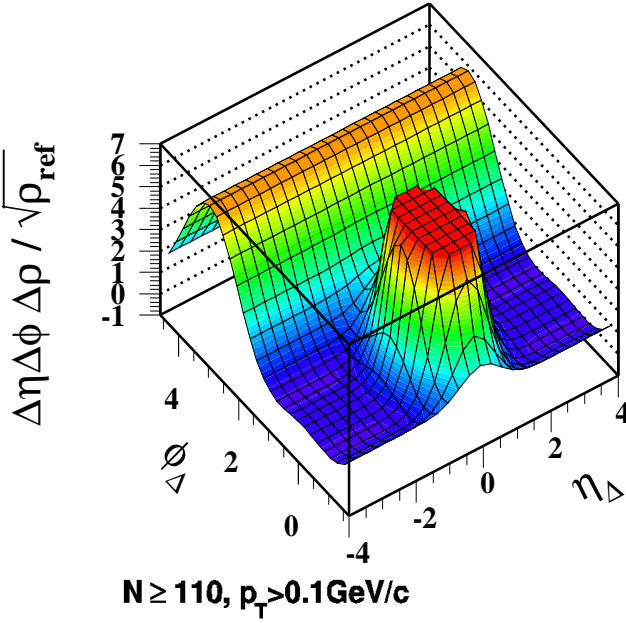


FIG. 4: Histograms from Fig. 3 rescaled by factor 5. Upper: Model function from Fig. 3 (left panel) but with quadrupole amplitude increased by factor 6 to $R_Q = 0.4$. Lower: CMS p_t -integral correlations for high-multiplicity cut [1].

FIG. 5: Upper: Model function from Fig. 4 (upper panel) with the same quadrupole amplitude but with jet correlation amplitudes and peak widths reduced (see text). Lower: CMS correlations for high-multiplicity cut and $p_t \in [1, 3]$ GeV/c [1].

application of multiplicity and p_t cuts. Is the unanticipated structure a signal of novel physics in LHC p - p collisions or a simple extrapolation from lower energies?

A. Comparison of multiplicity cuts

The $R(\sqrt{s})$ trend defined in Eq. (4) and inferred from angular correlation energy systematics below 200 GeV [11, 23] also describes NSD multiplicity densities well above 100 GeV. Given the NSD value $dN_{ch}/d\eta = 2.5$ at 200 GeV $R(\sqrt{s})$ predicts the value 5.75 at 7 TeV consistent with the recent CMS measurement ~ 5.8 [8].

The CMS high-multiplicity cut produced a 7-fold in-

crease over the NSD angular density ($dN_{ch}/d\eta = 40$ vs 5.8). In a STAR study of multiplicity dependence of 200 GeV p - p p_t spectra [7] the multiplicity range included a 10-fold increase ($dN_{ch}/d\eta = 25$ vs 2.5). The maximum particle density at 200 GeV was thus 60% of the maximum at 7 TeV—less than a factor two difference.

B. Minijet cut systematics

a. Multiplicity cut In Sec. VB we concluded that application of the CMS high-multiplicity cut results in an increase in the jet correlation amplitude by about a factor 3. Our experience with 200 GeV jet correlations suggests

that the multiplicity cut acts to bias the jet frequency per collision, but that the minijet mean fragment multiplicity is not significantly biased (the multiplicity cut does not alter minimum-bias parton fragmentation) [7].

In Sec. IV E we noted that with a ten-fold increase in event multiplicity the jet frequency in 200 GeV p - p collisions increases by about a factor 50, and the jet correlation amplitude increases by a factor 5. The increase saturates when the jet probability nears 100%. At 7 TeV the minimum-bias jet frequency increases by factor $R(7 \text{ TeV}) = 2.3$ to almost 5%. The maximum frequency increase is then $50/2.3 = 22$. With a 7-fold increase in multiplicity we expect the correlation amplitude to increase by a factor 3, which we observe in the CMS data.

b. p_t cuts In 200 GeV p - p correlations on $y_t \times y_t$ [14, 15] we observe that SS jet correlations extend down to 0.3 GeV/c, with mode at 1 GeV/c. Nearly half the SS correlated pairs appear below the mode. In contrast, AS correlations are cut off near 0.7 GeV/c. The cutoff is attributed to k_t effects. As a consequence a smaller fraction of AS pairs appears below 1 GeV/c. In Sec. V C we note that for correlations corresponding to $p_t \in [1, 3]$ GeV/c the SS peak is reduced by factor 1/3 and the AS ridge is reduced by factor 1/2. Those results are consistent with 200 GeV jet structure on $y_t \times y_t$.

c. SS peak properties Minimum-bias SS peak properties for 7 TeV jet angular correlations are essentially identical to those at 200 GeV. With the high-multiplicity cut the SS peak azimuth width decreases from 0.9 to 0.65. With the additional high- p_t cut the azimuth width is further reduced to 0.55. 7 TeV SS peak trends are generally consistent with measurements at 200 GeV [14].

C. Quadrupole systematics

The azimuth quadrupole in A-A collisions below 200 GeV depends only on collision energy and initial geometry, not on final-state particle density. The two trends are factorized, as in Eq. (5). Systematics for p - p collisions are inferred by analogy with A-A collisions. The quadrupole is insensitive to charge combination, with equal amplitude for LS and US charge pairs. Correspondence between azimuth quadrupole properties and the SS ridge observed in CMS data suggest that the “ridge” is in fact a manifestation of the azimuth quadrupole at 7 TeV.

a. Collision-energy systematics The azimuth quadrupole in Au-Au collisions at and below 200 GeV has a very simple parametrization [11], quite different from minijets which undergo a sharp transition on centrality [9]. Because the Au-Au centrality trend extends to peripheral N-N collisions extrapolation of the quadrupole amplitude to 200 GeV p - p collisions is fairly reliable. The parametrization includes a $\log(\sqrt{s})$ factor which can be extrapolated to predict the quadrupole for minimum-bias p - p collisions at 7 TeV.

b. Multiplicity and p_t cuts We expect selection of high-multiplicity p - p events to bias toward more-central

collisions. Arguing by analogy with A-A collisions increased multiplicity should then produce an increase in the quadrupole amplitude measured by $\rho_0 v_2^2$. The overall factor-six quadrupole amplitude increase with multiplicity inferred from CMS data is compatible with extrapolations based on available A-A data at 200 GeV.

A similar argument by analogy could be made for the consequences of p_t cuts. However, the systematics of p_t -differential $v_2(p_t, b)$ are rapidly changing for more-peripheral 200 GeV A-A collisions [12], implying large uncertainties for any extrapolation to p - p collisions. What we find empirically from comparisons of CMS results to 200 GeV minimum-bias correlations is that the CMS p_t cuts do not change the quadrupole amplitude significantly. The main effect of p_t cuts is to reduce the jet structure by a factor 2-3 relative to the fixed quadrupole amplitude, making the latter more visible.

c. Sensitivity to quadrupole in p - p collisions At 200 GeV the azimuth quadrupole is only marginally significant in p - p collisions. The quadrupole amplitude is better determined by extrapolation of the relation in Eq. (5) from more-peripheral A-A collisions. In minimum-bias p - p collisions at 7 TeV the quadrupole is not visually obvious but may be well-determined by model fits to data. With the imposition of multiplicity and p_t cuts the quadrupole becomes visually apparent, although the cuts produce only a six-fold amplitude increase.

The large data volumes and factor 2.3 amplitude increase with energy at the LHC may be combined with model fits to data to permit detailed exploration of azimuth quadrupole variations with multiplicity and p_t cuts in p - p collisions, leading to better understanding of the azimuth quadrupole as a QCD phenomenon.

D. The “ridge” at RHIC and LHC

The so-called “ridge” phenomenon at RHIC has two aspects which should be distinguished: (i) η elongation of a monolithic SS jet peak well described by a single 2D Gaussian [5, 9] and (ii) claimed development of a separate ridge-like structure beneath a symmetric 2D jet peak [2]. Item (i), well established for untriggered (no p_t cuts) jet correlations and for some combinations of p_t cuts, has been referred to as the “soft ridge,” although there is no separate ridge per se. Item (ii) is inferred from other combinations of p_t cuts (“triggered” analysis).

Elongation of the minimum-bias SS peak (i) undergoes a sharp transition on centrality in RHIC A-A collisions (both Au-Au and Cu-Cu collisions) [9]. For more-peripheral and p - p collisions the SS peak is strongly elongated in the ϕ direction (3:2) [15]. For more-central collisions the SS peak becomes strongly elongated in the η direction (3:1) [5, 9]. The transition occurs within a small centrality interval. The mechanism is an open question.

Variation of SS jet peak structure with p_t cuts is complex, depending on the details of fragmentation for different charge-sign combinations, fragment p_t s and hadron

species. Such details are currently poorly explored. Assignment of certain aspects of peak structure to a distinct ridge phenomenon for some p_t cuts (ii) is questionable.

For the CMS data we observe that the SS 2D peak η width at 7 TeV has the same value as that at 0.2 TeV and is reduced slightly with applied cuts. Thus, η broadening, item (i) observed at RHIC, is not present. The azimuth width varies with cuts just as in 200 GeV p - p collisions.

The appearance of a SS “ridge” in CMS data for some cut combinations is attributed to item (ii) above, given the apparent similarity. However, the absence of item (i) and consistency with known azimuth quadrupole systematics makes interpretation (ii) less likely. A more definitive answer will come with systematic study of Pb-Pb centrality systematics in upcoming LHC heavy ion runs: How does the sharp transition vary with collision energy?

Interpretation of the SS “ridge” at 7 TeV as a manifestation of the azimuth quadrupole does not imply that “elliptic flow” is present in p - p collisions. Instead, appearance of the quadrupole in elementary collisions is consistent with evidence against a hydrodynamic interpretation in more-central A-A collisions [16, 27, 28]. Recent results suggest that the quadrupole is a novel QCD phenomenon which should be studied as such [24].

VII. SUMMARY

Direct comparison of angular correlations indicates that there is remarkably little difference between 0.2 TeV and 7 TeV NSD p - p collisions. Midrapidity correlation amplitudes and multiplicity density increase by factor $R(\sqrt{s} = 7 \text{ TeV}) = 2.3$ over those measured at 0.2 TeV. The minimum-bias correlation structure is otherwise quite similar given present measurement accuracy.

Response to multiplicity and p_t cuts is also consistent with trends at 0.2 TeV. The change in jet correlation amplitude and same-side 2D jet peak properties is as expected from STAR correlation analysis at 0.2 TeV. The single novel manifestation at the LHC is the appearance of a same-side “ridge” for certain multiplicity and p_t cuts. It is conjectured that the ridge structure in 7 TeV p - p collisions may be similar to that observed in more-central Au-Au collisions at 0.2 TeV, interpreted by some to indicate formation of a dense, flowing QCD medium.

However, extrapolation of azimuth quadrupole systematics measured in A-A collisions at 0.2 TeV to 7 TeV predicts a substantial quadrupole amplitude in minimum-bias p - p collisions. Although the consequences for the quadrupole of multiplicity and p_t cuts applied in the CMS analysis cannot be predicted quantitatively from present 0.2 TeV results a modest six-fold increase over the minimum-bias quadrupole prediction fully accounts for the same-side ridge structure in 7 GeV p - p collisions.

We conclude that by a combination of larger collision energy, kinematic cuts and large event numbers the azimuth quadrupole apparent in more-central A-A collisions at RHIC is directly visualized in p - p angular correlations at the LHC. LHC p - p data then offer the possibility to study the systematics of the azimuth quadrupole in elementary collisions. Model fits can be applied as in the cited references to increase sensitivity to quadrupole structure. By such means the azimuth quadrupole may be better understood as a QCD phenomenon.

We greatly appreciate lengthy discussions on two-particle correlations in nuclear collisions over a number of years with Lanny Ray, Jeff Porter and Duncan Prindle. This work was supported in part by the Office of Science of the U.S. DOE under grant DE-FG03-97ER41020.

-
- [1] CMS Collaboration, JHEP **1009**, 091 (2010), arXiv:1009.4122.
 - [2] B. I. Abelev *et al.* (STAR Collaboration), Phys. Rev. C **80**, 064912 (2009).
 - [3] T. Hirano and M. Gyulassy, Nucl. Phys. A **769**, 71 (2006).
 - [4] L. P. Csernai, J. I. Kapusta and L. D. McLerran, Phys. Rev. Lett. **97**, 152303 (2006).
 - [5] J. Adams *et al.* (STAR Collaboration), Phys. Rev. C **73**, 064907 (2006).
 - [6] J. Adams *et al.* (STAR Collaboration), Phys. Lett. B **634**, 347 (2006).
 - [7] J. Adams *et al.* (STAR Collaboration), Phys. Rev. D **74**, 032006 (2006).
 - [8] V. Khachatryan *et al.* (CMS Collaboration), Phys. Rev. Lett. **105**, 022002 (2010).
 - [9] M. Daugherty (STAR Collaboration), J. Phys. G **35**, 104090 (2008).
 - [10] T. A. Trainor, R. J. Porter and D. J. Prindle, J. Phys. G **31**, 809 (2005).
 - [11] D. T. Kettler (STAR collaboration), Eur. Phys. J. C **62**, 175 (2009).
 - [12] D. Kettler (STAR Collaboration), arXiv:1008.4793.
 - [13] R. J. Porter and T. A. Trainor (STAR Collaboration), Acta Phys. Polon. B **36**, 353 (2005).
 - [14] R. J. Porter and T. A. Trainor (STAR Collaboration), J. Phys. Conf. Ser. **27**, 98 (2005).
 - [15] R. J. Porter and T. A. Trainor (STAR Collaboration), PoS C **FRNC2006**, 004 (2006).
 - [16] T. A. Trainor, Int. J. Mod. Phys. E **17**, 1499 (2008).
 - [17] T. A. Trainor and D. T. Kettler, arXiv:1008.4759.
 - [18] X.-N. Wang, Phys. Rev. D **46**, R1900 (1992); X.-N. Wang and M. Gyulassy, Phys. Rev. D **44**, 3501 (1991).
 - [19] C. Albajar *et al.* (UA1 Collaboration), Nucl. Phys. B **309**, 405 (1988).
 - [20] T. A. Trainor, Phys. Rev. C **80**, 044901 (2009).
 - [21] T. A. Trainor, Phys. Rev. C **81**, 014905 (2010).
 - [22] J. Adams *et al.* (STAR Collaboration), J. Phys. G **32**, L37 (2006).
 - [23] J. Adams *et al.* (STAR Collaboration), J. Phys. G **33**, 451 (2007).
 - [24] T. A. Trainor, Mod. Phys. Lett. A **23**, 569 (2008).

- [25] P. Huovinen and P. V. Ruuskanen, Ann. Rev. Nucl. Part. Sci. **56**, 163 (2006).
- [26] L. Frankfurt, M. Strikman and C. Weiss, Phys. Rev. D **69**, 114010 (2004).
- [27] T. A. Trainor, Phys. Rev. C **78**, 064908 (2008).
- [28] T. A. Trainor, J. Phys. G **37**, 085004 (2010).